Supporting information on

Tubular nitrogen-doped TiO_2 samples with efficient photocatalytic properties based on long-lived charge separation under visible-light irradiation: synthesis, characterization and reactivity

Yoshikazu Hirose,[a] Atsushi Itadani,[a,†] Takahiro Ohkubo,[a] Hideki Hashimoto,[b,‡] Jun Takada,[b] Shigeharu Kittaka[c] and Yasushige Kuroda [*,a]

[a]*Department of Chemistry, Graduate School of Natural Science and Technology, Okayama University, 3-1-1 Tsushima, Kita-ku, Okayama 700-8530, Japan* ,[b]*Department of Applied Chemistry, Graduate School of Natural Science and Technology, Okayama University, 3-1-1 Tsushima, Kita-ku, Okayama 700-8530, Japan, and* [c]*Department of Chemistry, Faculty of Science, Okayama University of Science, 1-1 Ridaicho, Kita-ku, Okayama 700-0005, Japan.*

† & ‡ Present address:

[†]Graduate School of Science and Technology, Niigata University, 8050 Ikarashi, 2-no-cho, Nishi-ku, Niigata, 950-2181, Japan

[‡]Department of Applied Chemistry, School of Advanced Engineering, Kogakuin University, Hachioji 192-0015, Japan.

Captions to the Figures in the Supporting information:

Figure SI-1. Adsorption isotherms of N_2 and the resulting pore-size distribution curvess on each sample. (a, b) Nitrogen adsorption-desorption isotherms, (c, d) pore-size distributions. (a, c) as prepared (before calcinations) samples, (b, d) samples calcined at 573 K. To understand easily the relation, each curve is shifted by 100 cm^3 (S.T.P) g^{-1} in the Y-axis data relating to the adsorption isotherms. (1) T-TiO_2; (2) T-$TiO_{2-\delta}N_\delta$(A); (3) T-$TiO_{2-\delta}N_\delta$(B); (4) T-$TiO_{2-\delta}N_\delta$(C).

Figure SI-2. IR spectra for respective as-prepared samples: (a) T-$TiO_{2-\delta}N_\delta$(A); (b) T-$TiO_{2-\delta}N_\delta$(C). The samples were evacuated at various temperatures: (1) 300, (2) 373, (3) 423, (4) 473, (5) 523, (6) 573, and (7) 623 K, respectively.

Figure SI-3. Difference IR spectra for respective samples: (a) T-TiO_2, (b) T-$TiO_{2-\delta}N_\delta$(A), (c) T-$TiO_{2-\delta}N_\delta$(B), (d) T-$TiO_{2-\delta}N_\delta$(C). The samples were evacuated at various temperatures and the following difference spectra between following temperatures were given: (1) (373 K- 300 K), (2) (423 K- 373 K), (3) (473 K-423 K), (4) (523 K- 473 K), (5) (573 K - 523 K), and (6) (623 K-573 K), respectively.

Figure SI-4. EPR spectra of the samples calcined at 573 K: (1) T-TiO_2; (2) T-$TiO_{2-\delta}N_\delta$(A); (3) T-$TiO_{2-\delta}N_\delta$(B); (4) T-$TiO_{2-\delta}N_\delta$(C). The respective samples were treated with visible-light irradiation in the presence of O_2. The signals around 332.9 and 341.5 mT were determined on the basis of the bands observed in the Mn^{2+}/MgO sample as a reference.

Figure SI-5. IR spectra of respective samples: (a) T-TiO_2 and (b) T-$TiO_{2-\delta}N_\delta$(A). Each sample was first calcined at 573 K and then re-evacuated at 300 K in in-situ cell for IR measurements. On which various treatments were carried out. In both figures, the difference spectra in respective stages with respect the reference state of the sample which was calcined at 573 K and then evacuated at 300 K are shown: (1) visible light irradiation in vacuo, (2) equilibrated with O_2 gas under a pressure of 20 kPa at 300 K, (3) visible light irradiation in the O_2 atmosphere, and (4) evacuated at 300 K after measurement of the spectrum 3.

Figure SI-1. Y. Hirose, et al.,

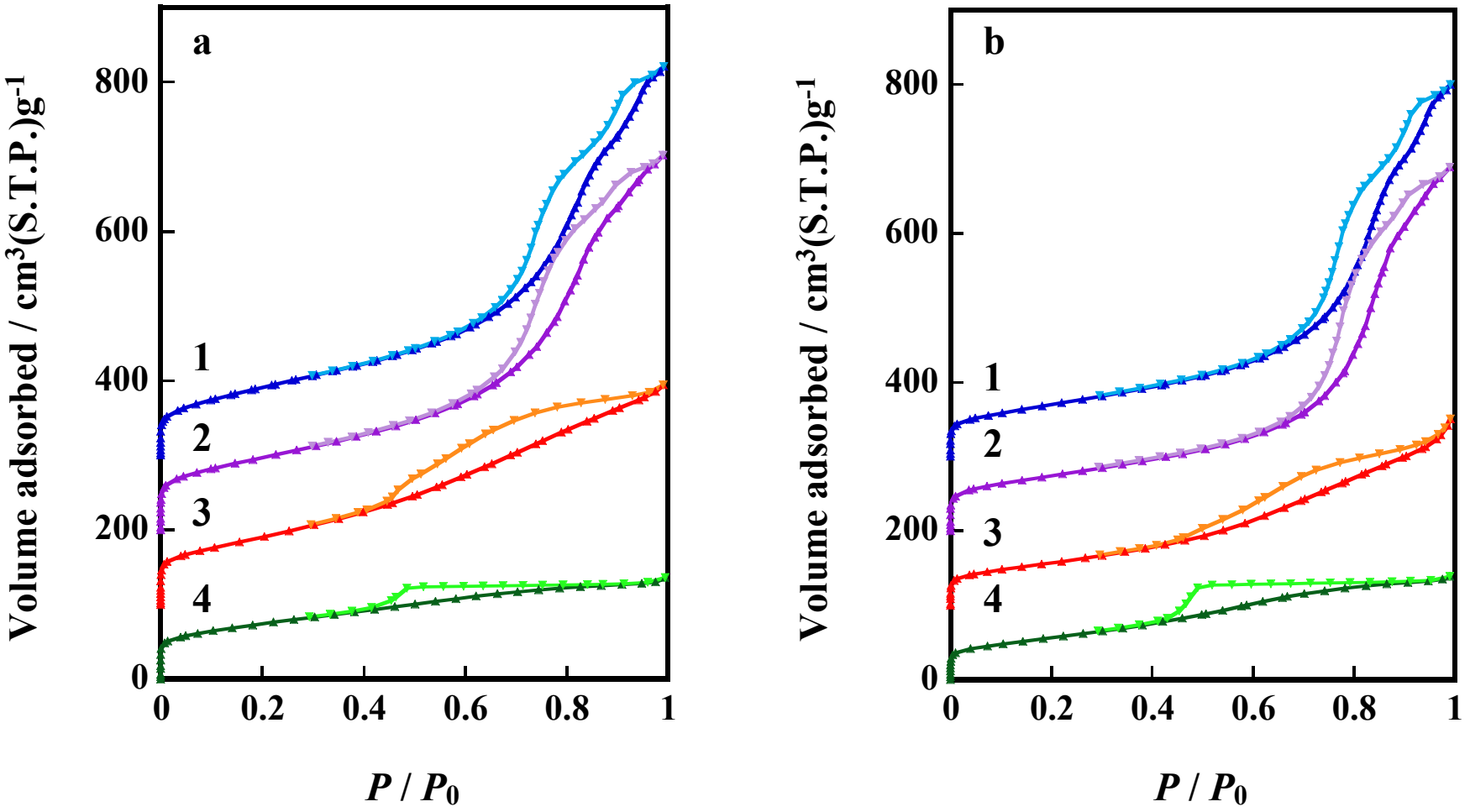

Figure SI-1. Continued, Y. Hirose, et al.,

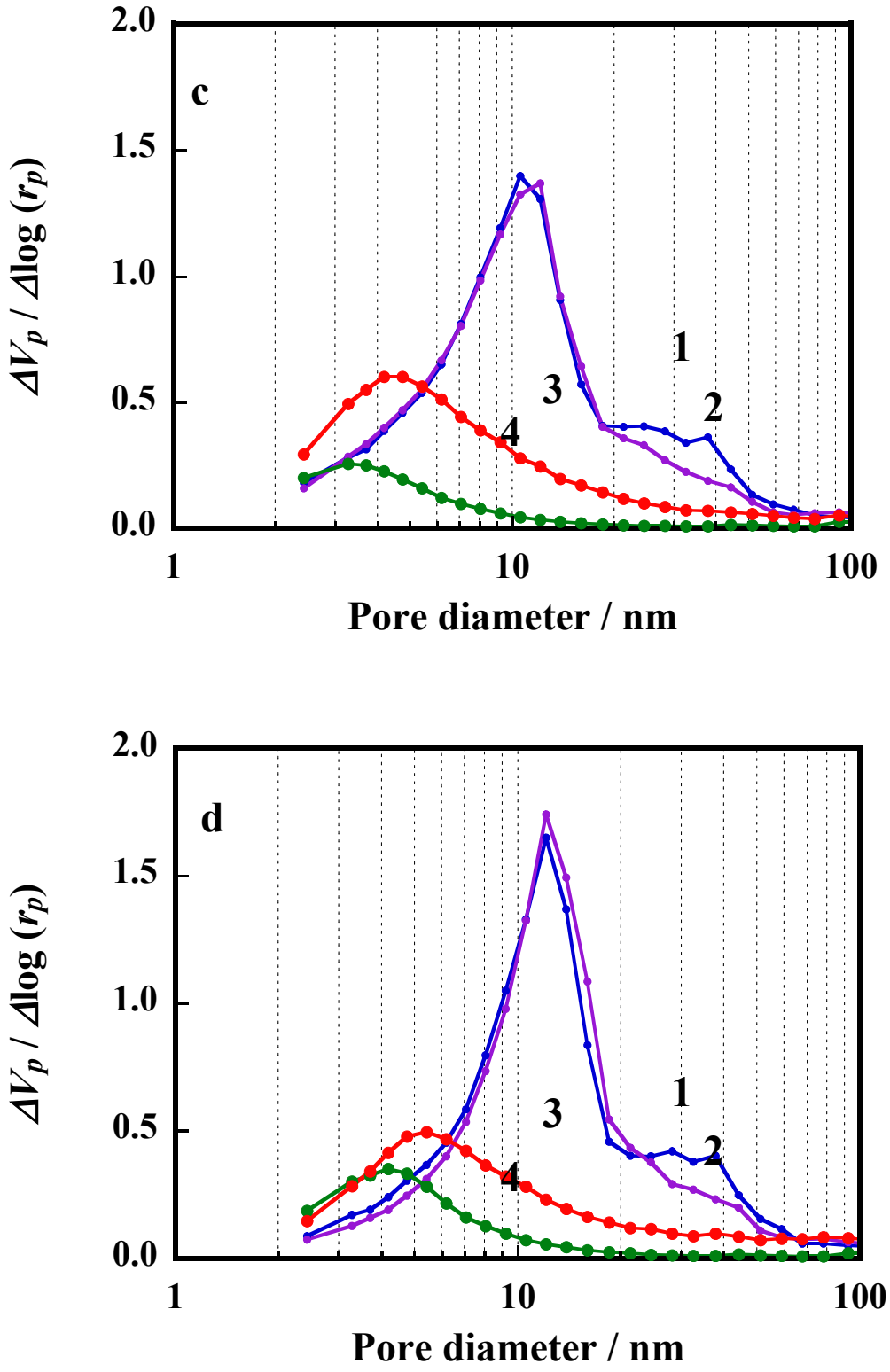

Figure SI-2. Y. Hirose, et al.,

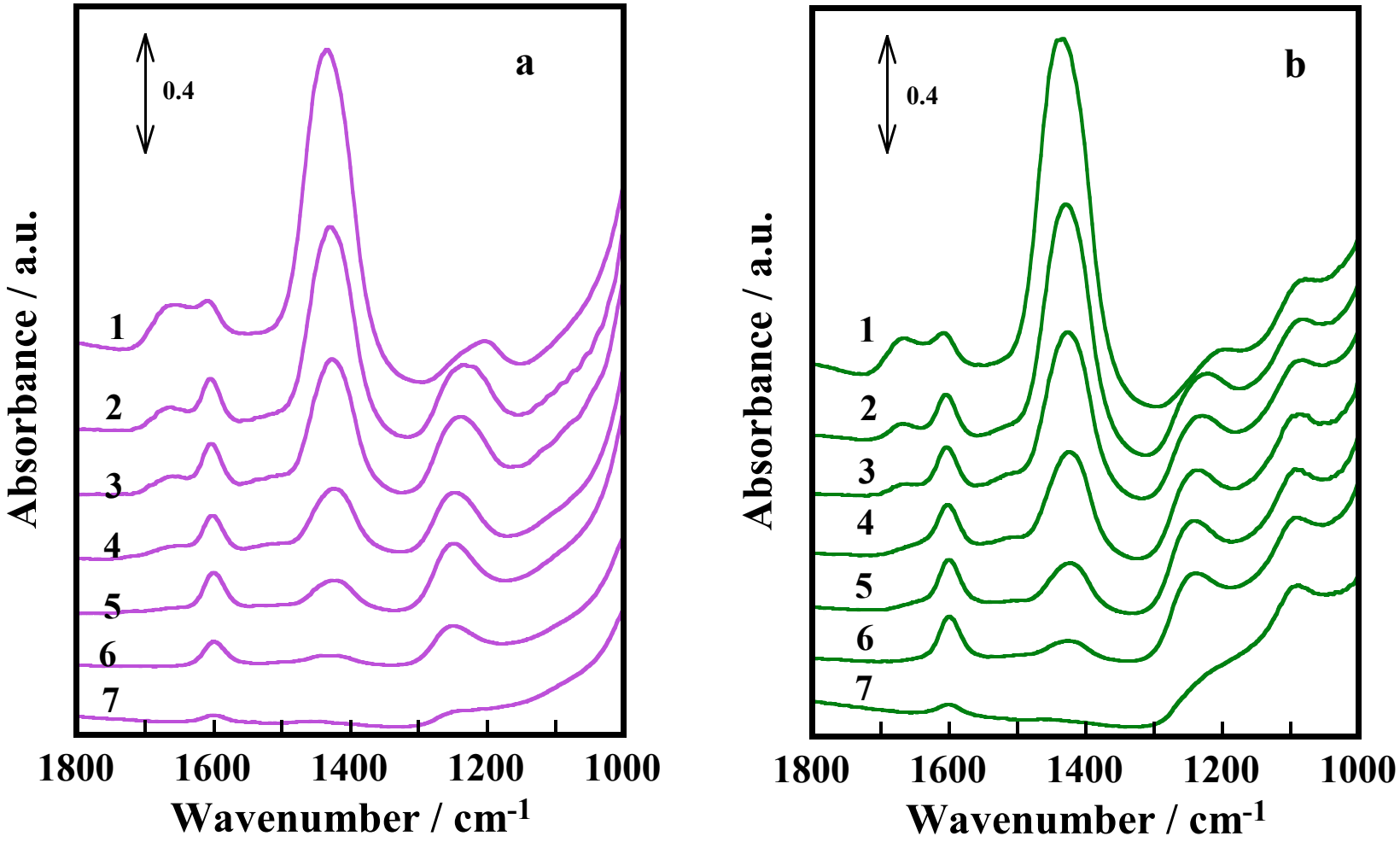

Figure SI-3. Y. Hirose, et al.,

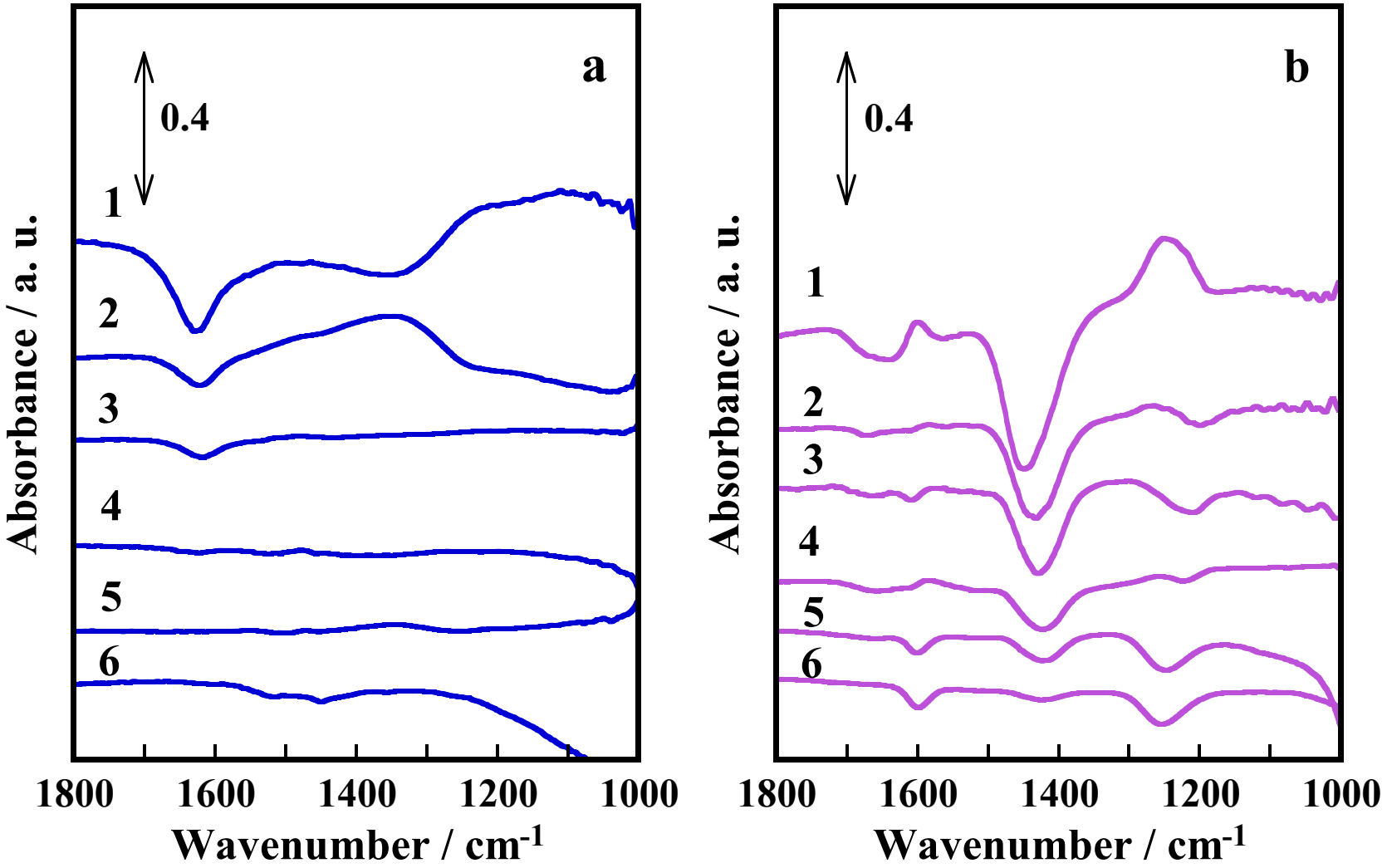

Figure SI-3. Continued, Y. Hirose, et al.,

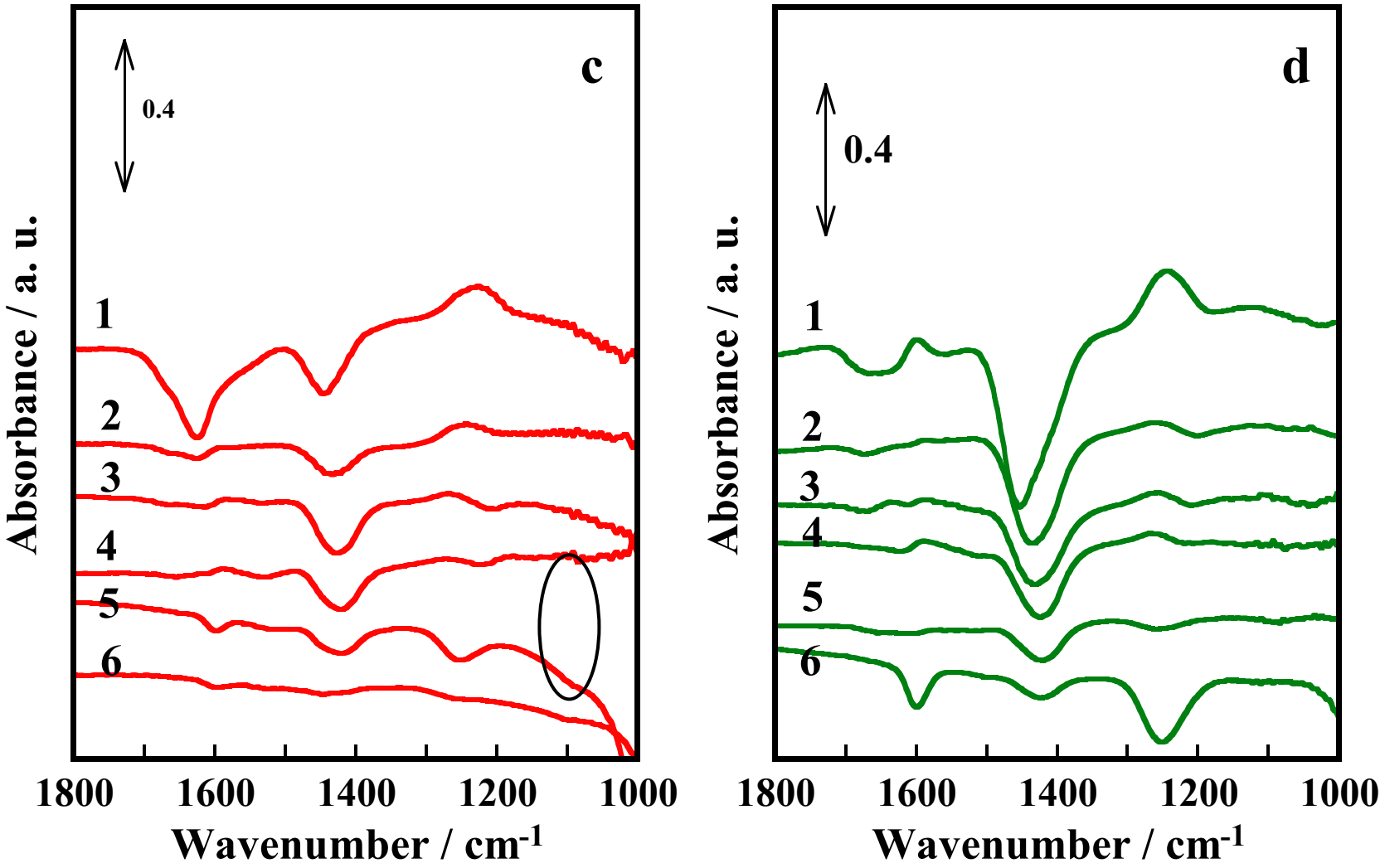

Figure SI-4. Y. Hirose, et al.,

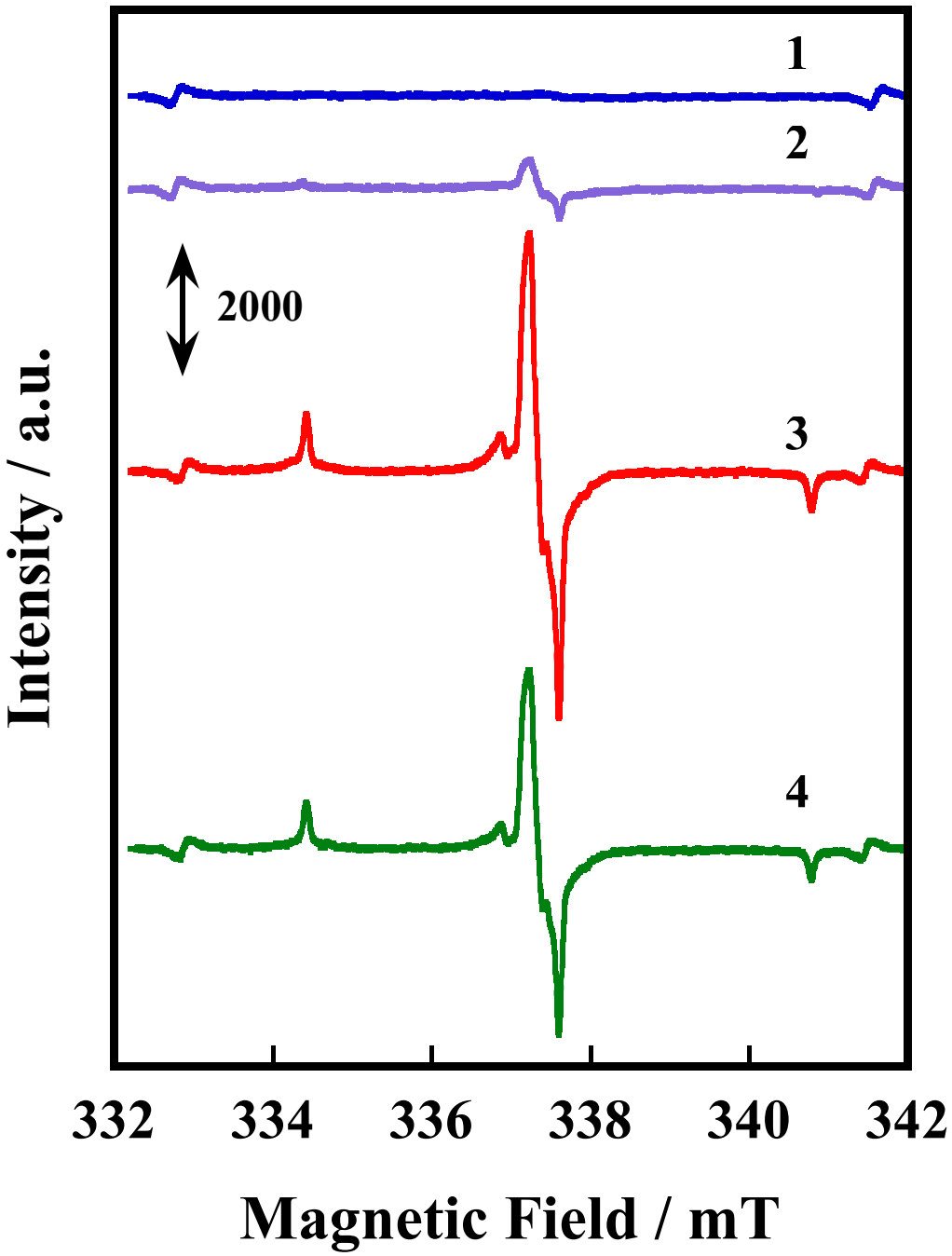

Figure SI-5. Y. Hirose, et al.,